A newly identified prophage-encoded gene, *ymfM*, causes SOS-inducible filamentation in *Escherichia coli*

Shirin Ansari[a,b*], James C. Walsh[b], Amy L. Bottomley[a], Iain G. Duggin[a], Catherine Burke[a], Elizabeth J. Harry[a,#]

[a] The ithree institute, Faculty of Science, University of Technology Sydney, Sydney, Australia

[b] EMBL Australia Node in Single Molecule Science and ARC Centre of Excellence in Advanced Molecular Imaging, School of Medical Sciences, University of New South Wales, Sydney, Australia

Running title: SOS-inducible filamentation by gene, *ymfM*.

[#] Address correspondence to Elizabeth J. Harry; Elizabeth.Harry@uts.edu.au

*Present address

Abstract:

Rod-shaped bacteria such as *Escherichia coli* can regulate cell division in response to stress, leading to filamentation, a process where cell growth and DNA replication continues in the absence of division, resulting in elongated cells. The classic example of stress is DNA damage which results in the activation of the SOS response. While the inhibition of cell division during SOS has traditionally been attributed to SulA in *E. coli*, a previous report suggests that the e14 prophage may also encode an SOS-inducible cell division inhibitor, previously named SfiC. However, the exact gene responsible for this division inhibition has remained unknown for over 35 years. A recent high-throughput over-expression screen in *E. coli* identified the e14 prophage gene, *ymfM*, as a potential cell division inhibitor. In this study, we show that the inducible expression of *ymfM* from a plasmid causes filamentation. We show that this expression of *ymfM* results in the inhibition of Z ring formation and is independent of the well characterised inhibitors of FtsZ ring assembly in *E. coli*, SulA, SlmA and MinC. We confirm that *ymfM* is the gene responsible for the SfiC phenotype as it contributes to the filamentation observed during the SOS response. This function is independent of SulA, highlighting that multiple alternative division inhibition pathways exist during the SOS response. Our data also highlight that our current understanding of cell division regulation during the SOS response is incomplete and raises many questions regarding how many inhibitors there actually are and their purpose for the survival of the organism.

Importance:

Filamentation is an important biological mechanism which aids in the survival, pathogenesis and antibiotic resistance of bacteria within different environments, including pathogenic

bacteria such as uropathogenic *Escherichia coli*. Here we have identified a bacteriophage-encoded cell division inhibitor which contributes to the filamentation that occurs during the SOS response. Our work highlights that there are multiple pathways that inhibit cell division during stress. Identifying and characterising these pathways is a critical step in understanding survival tactics of bacteria which become important when combating the development of bacterial resistance to antibiotics and their pathogenicity.

Introduction:

Bacterial cell division is an essential process that is tightly regulated to ensure division occurs at the correct time and position in order to create two viable and genetically identical daughter cells (1). In *Escherichia coli* this begins with the accumulation of the essential protein, FtsZ, into a ring-like structure (Z ring), at mid-cell (2). Following this, several downstream division proteins are recruited to form a complex, known as the divisome, which then constricts to divide the cell in two (3). There are several regulatory mechanisms that underlie the timing and positioning of division in *E. coli.* This includes the well-characterized Min system, which prevents the formation of Z rings at the cell poles, and the nucleoid occlusion protein, SlmA, which inhibits Z-ring formation over unsegregated DNA (4, 5).

In addition to ensuring correct timing and positioning of the division site, there are numerous examples that demonstrate that the inhibition of division is equally important for cell survival under conditions such as DNA damage, protection from predation, progression of infection and pathogenesis (6-8). Inhibition of division results in the formation of filamentous cells; a process where cell growth and DNA replication continue in the absence of division, resulting in elongated cells (6). Filamentation is an important survival mechanism utilised by several bacteria in response to environmental stimuli (6, 8).

A well characterised cellular pathway that leads to filamentation is the SOS response which is activated by DNA damage under conditions including oxidative stress, antibiotic treatment or UV exposure (9). The activation of the SOS response is coordinated by two regulatory proteins, RecA and LexA (10, 11). RecA binds to single-stranded DNA (ssDNA) breaks caused by DNA damage, forming a RecA-DNA filament, which facilitates the self-cleavage of the LexA repressor, and the subsequent up-regulation (de-repression) of LexA-controlled genes (12). LexA represses over 40 genes in *E. coli* under normal growth conditions (13).

A key function of the SOS response is to inhibit cell division. This is thought to allow sufficient time for DNA repair to occur before committing to producing the next generation of daughter cells, minimising the transmission of defective DNA (14). In *E. coli*, this is facilitated by the cell division inhibitor, SulA, which is under the regulatory control of LexA (9). SulA is perhaps one of the most studied cell division inhibitors that causes filamentation, with molecular studies showing that it directly interacts with FtsZ, preventing assembly of the Z ring (15-19). When DNA damage is repaired, SulA is degraded via the cytoplasmic protease, Lon, and FtsZ polymerisation and cell division resumes (20, 21).

While SulA is generally the only cell division inhibitor commonly attributed to cell division inhibition during the SOS response in *E. coli*, other cell division inhibitors have been identified in this organism. Interestingly, several of these inhibitors include genes encoded within prophages (22-26). The e14 prophage contains an unidentified SOS-inducible cell division inhibitor, previously named SfiC, which has been shown to contribute to filamentation during the SOS response, independent of SulA (27, 28). This inhibitor was not however under LexA repression (27). Phages contain their own repressor systems, which are

LexA-like in nature, such as the CI-repressor from λ phage (13, 29). The gene *cohE* from e14, encodes a CI-like repressor, similar in sequence to other bacteriophage CI repressors that are responsive to an SOS signal (30). As such, it is possible that expression of *sfiC* is regulated by *cohE*. In earlier work, it was also shown that FtsZ was most likely the target of SfiC, as point mutations in *ftsZ* that confer resistance to the inhibitory effects of SulA, also conferred resistance to SfiC (27, 28). Based on prophage arrangement, the gene responsible for the SfiC phenotype has been suggested to be likely encoded by either of the adjacent e14 prophage genes *ymfL* or *ymfM* (30), however the precise identity of the gene remains unknown.

We previously developed a high-throughput flow cytometry system to screen a novel *E. coli* expression library for candidate cell division regulators (31). We identified a DNA fragment containing the e14 prophage-encoded genes, the full *ymfM* gene and a partial sequence of adjacent genes, *ymfL* and *oweE* (previously annotated as *ymfN*), that when expressed in an inducible plasmid-based system, caused cells to elongate and form filaments (31, 32). Since this DNA fragment contained both potential candidates for SfiC, *ymfM and ymfL*, further work was needed to determine which of these genes is responsible for the SfiC phenotype i.e. SulA-independent filamentation during the SOS response.

Here we show that *ymfM* is responsible for the SfiC phenotype, resulting in the inhibition of cell division when expressed from an inducible plasmid. We further characterise the effect of *ymfM* expression on *E. coli* cell division and show that it results in prevention of the early stage of cell division: Z-ring formation. Furthermore, its inhibition pathway is independent of known cell division inhibitors, SulA, SlmA and MinC. Finally, we show that YmfM causes filamentation during activation of the SOS response and that this is independent of SulA.

126 Our data indicate that multiple division inhibitors exist during the SOS response and raises
127 questions regarding their purpose for the survival of *E. coli* during times of stress.

128 **Results**

129

130 **1. Identification of a new gene, *ymfM*, whose expression induces filamentation:**

131 Previous independent theoretical (30) and experimental (27, 31) studies have identified that
132 either *ymfM* or *ymfL*, is *sfiC*. To determine which one of these genes is responsible for the
133 SfiC filamentous phenotype, *ymfM* and *ymfL* were cloned separately into the arabinose-
134 inducible plasmid, pBAD24. Cells were grown in LB supplemented with 0.2% glucose to
135 mid-exponential phase to repress gene expression. The cells were then diluted in fresh LB
136 supplemented with 0.2% arabinose to induce gene expression and then grown for at least 4
137 doubling times (generation time is approximately 30 minutes) to allow for enough time to
138 observe cell length changes. The degree of filamentation associated with the expression of
139 each individual gene was measured as cell length (µm) from phase-contrast microscopy
140 images. Control cells expressing just pBAD24 had an average cell length of 4.2 ± 1.5 µm,
141 and these ranged from approximately 2 µm to 10 µm in length (Figure S1). Therefore,
142 filamentous cells resulting from gene expression in pBAD24 were defined as being greater
143 than 10 µm in cell length.

144

145 The induction of *ymfL* expression did not cause filamentation, with cells having an average
146 length of 3.5 ± 0.9 µm (Figure 1A). However, expression of *ymfM* resulted in inhibition of
147 division, giving rise to an exclusively filamentous population having an average cell length of
148 57.3 ± 19.7 µm (Figure 1B). In the repressed state, cells had the same cell-length distribution
149 as the empty vector (Figure 1 and S1). The initial doubling time was 30 min, which for the
150 120-min total incubation would result in filamentous cells 16-fold (2^4) longer than their short-

cell counterpart. The mean length of *ymfM*-induced cells was 14.5 times the *ymfM*-repressed mean of 3.9 µm. Overall these results identify conclusively that *ymfM* is the gene responsible for the filamentation observed in the *E. coli* overexpression screen (31) and in the SfiC phenotype (27).

2. *ymfM* expression inhibits the earliest stage of division: FtsZ ring formation

To understand whether induction of *ymfM* expression inhibits cell division by impeding FtsZ assembly or a later stage of cell division, immunofluorescence microscopy (IFM) was used to measure Z ring frequency in cells induced to express *ymfM* from pBAD24. The absence of Z rings in the *ymfM*-induced cells would imply that Z ring formation has been inhibited.

IFM using cephalexin-treated filamentous cells was first performed as a control to show that the technique did not affect the integrity of the Z rings in filaments, and other control experiments showed that the antibody detection for IFM is specific for FtsZ (Figure S2).

Next, wild-type cells harbouring pBAD-*ymfM* were grown in LB for 3 generations with either glucose to repress expression or with arabinose to induce expression for 90 min. During repressed conditions, cells had an average cell length of 3.5 ± 0.9 µm indicating that they were dividing at the normal frequency. In these short cells, Z rings were observed as bright green bands at mid-cell (white arrow, Figure 2). The numbers of Z rings were scored from visual inspection of approximately 100 cells. For each cell, the cell length was also measured from the image. The frequency of Z ring observation calculated by dividing the total length of all cells counted by the total number of Z rings observed (µm/Z ring). In the short cell population Z rings were observed at a frequency of 8.4 µm/Z ring. In cells expressing *ymfM*, the average cell length was 35.5 ± 23.1 µm and almost no Z rings were

observed along the length of the filament. Instead FtsZ appeared to be diffused throughout the filament (Figure 2B). Occasional Z rings were seen in this sample; however these were primarily in the few short cells present. Z rings in this population were observed at a frequency of 224 µm/Z ring – 27-fold less frequent compared to repressed cells. DAPI (DNA) staining showed that in *ymfM*-induced filaments, that the nucleoids appeared normal, suggesting that the filamentation observed is solely due to the inhibition of division and not a result of inhibition of DNA replication or chromosome segregation. Furthermore, it was shown that the lack of Z rings in filaments was not due to changes in cellular levels of FtsZ (Figure S3), indicating that YmfM does not prevent Z ring formation by proteolysis or degradation of FtsZ.

In summary, induced expression of *ymfM* results in inhibition of Z ring formation at midcell and this inhibition is likely affecting FtsZ mechanistically as cellular levels of FtsZ are not affected.

3. YmfM inhibition of division does not rely on known cell division regulators, SulA, SlmA and MinC

Induced expression of *ymfM* inhibits the earliest stage of division as Z rings were not detected with IFM (Figure 2). We next tested whether this inhibition occurred through other Z ring regulators. These include SulA, which inhibits FtsZ from assembling into a ring during the SOS response (15, 16); MinC, which prevents FtsZ assembly at cell poles under normal conditions (33, 34); and SlmA, which prevents FtsZ assembly over nucleoids as part of the nucleoid occlusion system in *E. coli* (35, 36). The expression of *ymfM* was induced in *E. coli* cells in the absence of SulA, (Δ*sulA*; JW0941) (37), SlmA (Δ*slmA*; JW5641) (37) or the Min system (Δ*minCDE*;TB43) (35). If YmfM prevents Z ring assembly specifically via any one of

these other inhibitors, then no filamentation will be observed in their absence when *ymfM* is expressed.

When *ymfM* expression was repressed, the mutant strains had a short cell distribution which was comparable to their wild-type counterpart, except for Δ*minCDE*. The absence of the Min proteins is reported to cause a mixed population of minicells (small cells lacking DNA) and mildly filamentous cells due to polar cell division (15) and this was observed in the Δ*minCDE* cell population. Cell lengths were 3.9 ± 1.2 µm (BW25113, parent of Δ*sulA* and Δ*slmA*), 3.8 ± 1.0 µm (Δ*sulA*), 5.7 ± 4.2 µm (Δ*slmA*), 4.3 ± 1.4 µm (TB28, parent to Δ*minCDE*) and 10.6 ± 5.5 µm (Δ*minCDE*).

When *ymfM* expression was induced in the mutant strains, Δ*sulA*, Δ*slmA* or Δ*minCDE*, filamentation was observed (Figure 3A and 3B). The average cell lengths were 71.8 ± 19.7 µm (Δ*sulA*), 70.6 ± 28.3 µm (Δ*slmA*) and 87.7 ± 16.1 µm (Δ*minCDE*), respectively. Filamentation in the mutant strains was comparable to their respective wild-type parent strain (Figure 3B), with average cell lengths of 76.2 ± 10.8 µm for BW25113 and 93.9 ± 15.4 µm for TB28. The results here show that *ymfM* does not require the inhibitory activity of SulA, SlmA or the Min system to inhibit Z ring formation.

4. YmfM is involved in the inhibition of division during the SOS response and is independent of SulA

Several years ago, an unknown gene, *sfiC*, was identified as a cell division inhibitor during the SOS response (27). D'Ari *et al*. (27) found that even in the absence of the *sulA* gene, cells were able to filament when SOS was activated as *sfiC* would inhibit cell division. We have thus far shown that *ymfM* is *sfiC*, as its expression from an inducible plasmid causes

filamentation (Figure 1) and this is independent of the inhibitory actions of SulA (Figure 3). *ymfM* therefore could also be responsible for the SulA-independent filamentation observed during the SOS response.

To show *ymfM* was required for filamentation during SOS in the absence of *sulA*, we used a similar approach to D'Ari et al (27), in which *sfiC* was identified using a temperature-sensitive mutant, *recA441*, also known as *recA-tif* (38). In this mutant, at the non-permissive temperature of 42^{o}C, constitutive protease activity of RecA is observed, thereby inducing the SOS response and filamentation without the need for external means to DNA damage (39). We therefore cloned *recA441* into pBAD24. Gene expression and subsequent SOS was induced with 0.2% arabinose and growth at 42^{o}C in strains Δ*ymfM*, Δ*sulA*, or Δ*sulA*Δ*ymfM.* Any changes to the degree of filamentation were measured. If, in the absence of *ymfM*, cells do not filament as effectively as their wild-type counterparts, this would suggest that *ymfM* directly contributes to filamentation during the SOS response.

As expected, induction of *recA441* caused filamentation in the wild-type background (Figure 4A, 4B, in green, and Figure 4C i) as compared to the short cell population of wild-type cells expressing empty vector (Figure 4A, 4B, in blue). Here, cell size (reported as μm^3) was measured using a Coulter cytometer and this is proportional to cell length as cell width is unchanged.

There was a reduction in the degree of filamentation in the absence of *sulA* alone (Figure 4A, 4B in red and Figure 4C ii), as compared to its wild-type counterpart. However, this did not fully recover to the short cell population (Fig. 4A, 4B, in blue), highlighting the presence of additional cell division inhibitor(s) that are active during the SOS response. The absence of

ymfM (Figure 4A ,4B, in yellow; Figure 4C iii) was similar to that of induction of *recA441* in wild-type cells (Figure 4A ,4B, in green), so the absence of *ymfM* alone does not result in less filamentation in the population. However, in the absence of both *sulA* and *ymfM* (Figure 4A, 4B, in purple; Figure 4C iv), there was the greatest shift towards the shorter cell population (blue line). The difference in cell size distribution of Δ*sulA*Δ*ymfM* (purple) cells compared to Δ*sulA* (red) cells shows that *ymfM* does indeed play a role in inhibiting division during the SOS response when r*ecA441* is induced and this role becomes evident when SulA is absent. Importantly, while the shift towards shorter cells was the greatest for Δ*sulA*Δ*ymfM* (purple), it did not lead to a full recovery to a short cell population (blue), suggesting the presence of additional SOS-inducible inhibitors in this organism. These trends were observed in multiple biological replicates (represented in Figure 4B and Figure S4).

Discussion

We have identified the gene, *ymfM*, which when expressed from an inducible plasmid causes arrest in cell division (Figure 1). YmfM is encoded within the e14 prophage which had been indicated to harbour the gene responsible for the SOS-inducible filamentation phenotype, SfiC (27, 28). The exact gene responsible for SfiC has remained elusive for over 35 years and was narrowed down to either *ymfL* or *ymfM* in 2004 (30). In this work, we eliminate *ymfL* and confirm *ymfM* as being responsible for the inhibition of division, confirming that *ymfM* is responsible for the filamentous SfiC phenotype reported in 1983 (27).

We first characterised the stage of division being inhibited by *ymfM*. The expression of *ymfM* inhibits Z ring formation as essentially no Z rings were seen in cells expressing *ymfM*. This is consistent with previous work by D'Ari *et al.*, (27) who demonstrated that mutations in *ftsZ* that confer resistance to the inhibitory effects of SulA also confer resistance to SfiC. We also

show that YmfM does not act through known *E. coli* cell division regulators, SulA, SlmA or MinC. Another phage-encoded inhibitor, DicB from prophage Qin has been reported to utilise the inhibitory actions of MinC as no filamentation by DicB was observed in the absence of the Min System (40, 41). Filamentation by YmfM was observed in the absence of *sulA*, *slmA* and *minCDE*, showing that it is independent of these inhibitory pathways. It remains to be seen whether *ymfM* targets FtsZ directly to inhibit Z ring assembly, or if it does so through early division proteins such as FtsA or ZipA (3), similar to the phage inhibitor, Kil (22, 42). Our data do not rule out the possibility that YmfM causes division inhibition indirectly through an as yet unidentified cell division inhibitor.

Since we have shown that induction of *ymfM* expression causes filamentation and is responsible for the SfiC phenotype, then, as an SOS-inducible gene, it should also contribute to filamentation when the SOS response is induced through the activation of RecA, as reported by D'Ari *et al* (27). This indeed was the case. Through activation of *recA441*, YmfM inhibited division during the SOS response (Figure 4). This was apparent when the degree of filamentation was compared between Δ*sulA* and Δ*sulA*Δ*ymfM*, as the double knockout resulted in shorter filaments as compared to Δ*sulA* alone. This observed difference in filamentation can be attributed to *ymfM*.

As the double knockout strain showed that *ymfM* is contributing to the filamentation seen in this assay, we expected that, similar to the *ΔsulA*, the absence of *ymfM* alone (*ΔymfM*) would also result in a slightly shorter cell population as compared to *wild-type* (Figure 4). However, this was not the case, and was unexpected given that induced expression of *ymfM* from pBAD-*ymfM* results in a strong filamentous phenotype (Figure 1B). This could be due to differences in expression levels of *ymfM* from the plasmid versus through SOS induction.

Furthermore, it is likely that in the SOS-induced system, as SulA is still present in the *ΔymfM* strain, SulA and potential additional cell division inhibitors are masking the phenotypic effects that can be caused by the absence of *ymfM*.

It was also apparent that genes additional to *sulA* and *ymfM* contribute to filamentation during RecA-activated SOS, as there was not a full recovery to a short-cell population in the Δ*sulA*Δ*ymfM* background (Figure 4B). Given that over 1000 genes are differentially expressed during the SOS response (43), it is likely that several SOS-inducible cell division inhibitors are yet to be identified. For example, KilR, another prophage-encoded cell division inhibitor, has only recently been shown to be activated by the small RNA, *oxyS*, in response to oxidative stress (44).

It is interesting to speculate why multiple cell division inhibitors are present during the SOS response and ask, how may they differ to SulA? Additionally, why are so many of these division inhibitors present in prophages? It has been shown that the 9 cryptic prophages present in *E. coli* K-12 are beneficial for survival and adaption under different environmental conditions and signals, including osmotic, oxidative and acid stress, biofilm formation and tolerance to antibiotics (28, 30, 45). Several of these prophages also encode cell division inhibitors such as Kil, DicB, DicF, and CbtA (23-26). K*ilR* from prophage Rac and *dicB* from prophage Qin are both cell division inhibitors which have been shown to be up-regulated during treatment with nalidixic acid and azlocillin and are thought to contribute to the resistance of these antibiotics (24, 25, 45). It is possible that these prophage-encoded inhibitors, originally serving the functions of the phage, have more recently been adapted to be induced in response to specific environmental cues for the benefit of the bacterium (45, 46).

It was of interest to us to understand conditions under which *ymfM* is active as this may help us differentiate how its function differs to that of SulA. Expression of *ymfM* is up-regulated during norfloxacin induced SOS (47-49). However, while we could also show that *ymfM* expression was upregulated under these conditions, we were repeatedly unable to show the requirement for this gene in causing filamentation in the presence of this antibiotic (data not shown) as we observed in the RecA441 experiments (Figure 4). As with the *recA441* experiments, we think it likely that the *ymfM* phenotype in the presence of norfloxacin is being masked by numerous filamentation mechanisms. Alternatively, since *ymfM* is not under the control of LexA repression (27), and likely controlled by the CI-like repressor within the e14 prophage, it possible that *ymfM* responds to different yet-to-be identified conditions. Like LexA, CI-repressors are responsive to SOS signals and are dependent on RecA-ssDNA binding to undergo auto-cleavage, resulting in expression of CI-repressed genes.

These observations also highlight the possibility that multiple cell division inhibitor genes and pathways exist for a more finely tuned division regulation response to the environment. For example, spatial inhibitors MinC and SlmA have specialised functions to ensure division does not occur at inappropriate times in the cell cycle or the incorrect position in the cell. It is probable that temporal inhibitors are equally specialised with respect to when they are activated. By having multiple inhibitors with subtly different properties, cells are likely able to tailor their inhibition in response to different environmental conditions and signals to maximise their survivability. More work is needed to tease apart the relationship between different inhibitors and the conditions under which they are required.

Overall, our data shows that *ymfM* is a novel gene required for cell division inhibition during the SOS response, and its activity is independent of a major SOS-induced cell division inhibitor, SulA. Our data also highlights that our current understanding of the cell division regulation during the SOS response is incomplete and raises many questions. In particular, what are the benefits of having multiple cell division inhibitors during the SOS response? How are the different inhibitors activated? And how do these multiple pathways help *E. coli* cope with stresses and aid in the survival of the population, if at all?

Methods and Materials

Strains and Growth Conditions

All *E. coli* strains used in this study are listed in Table S1. *E. coli* cells were grown in LB media with vigorous shaking (250 rpm) at 37^{o}C, unless stated otherwise. Ampicillin (100µg/mL; Sigma Aldrich) was supplemented, where appropriate. Lambda Red recombination (37, 50) was used to generate gene deletions in *E. coli* strains listed in Table S1.

Plasmid construction and expression

All plasmids used in this study are listed in Table S2. Recombinant plasmids were constructed using the Gibson assembly method (51) following the manufacturer's instructions for the Gibson assembly master mix (NEB). DNA fragments *ymfM*, *ymfL* and *oweE* were amplified from BW25113 genomic DNA and *recA441* was amplified from JM12 genomic DNA (38), see Table S3. Each DNA fragment contained homologous overlap to pBAD24 which was linearised at the *NcoI* restriction site.

Expression of DNA fragments from pBAD24

375 Cultures of desired *E. coli* strain containing recombinant pBAD24 were grown overnight in
376 5mL LB with ampicillin (100 µg/mL) and 0.2% glucose (repression of araBAD promoter) at
377 37°C, or 30°C for pBAD-*recA441*. Cultures were diluted to OD_{600} = 0.04 in 20mL LB with
378 ampicillin (100 µg/mL) and 0.2% glucose and grown at 37°C (or 30°C for pBAD-*recA441*),
379 250 rpm to mid-exponential phase (OD600 ~ 0.5). A 1mL aliquot of the culture was collected
380 and fixed with 3% formaldehyde. Remainder of the culture was pelleted by centrifugation at
381 2, 000 x *g*, and washed twice in an equal volume of fresh LB to remove the glucose. Cultures
382 were further diluted to an OD_{600}=0.04 in 20mL LB with ampicillin (100 µg/mL) and 0.2%
383 arabinose (to induce expression) and grown for 4 generations (approximately 2 hours) at
384 37°C with shaking. For *recA441* expression, cultures were grown at 42°C and supplemented
385 with 100 µg/mL adenine in addition to the arabinose and ampicillin.
386
387 **Microscopy**
388 **Immunofluorescence microscopy (IFM)**
389 IFM was used for the detection of the FtsZ protein and is based on the method previously
390 described in (52), with the exception that cell lysis was omitted. Cultures of BW25113
391 containing pBAD-*ymfM* were grown as detailed above and incubated with the primary
392 antibody, αFtsZ (anti-sera), diluted 1:10,000 in BSA-PBS, at 4°C overnight. The primary
393 antibody was removed, and the cells were incubated with Alexa488-conjugated secondary
394 antibody, αRabbit IgG (Invitrogen), diluted 1: 10,000 in BSA-PBS, for 2 hours in the dark, at
395 room temperature. Wells were washed with PBS to remove excess secondary antibody and
396 DAPI (4'6-diamidino-2-phenylindole), at a final concentration of 2µg/mL was added to each
397 sample. Cell morphology and FtsZ localisation was then examined using phase-contrast and
398 fluorescence microscopy as described below.
399

400 **Phase-contrast and Fluorescence Microscopy**

401 Cells were imaged using phase-contrast and fluorescence on a Zeiss Axioplan 2 fluorescent
402 microscope equipped with a Plan Apochromat (100x NA 1.4; Zeiss) objective lens. The light
403 source was a 100 W high pressure mercury lamp passed through the following filter blocks
404 for visualising Alexa Fluor 488 (Filter set 09, Zeiss; 450 – 490 nm BP excitation filter, 515
405 nm long pass (LP) barrier filter), and for visualising DAPI (Filter set 02, Zeiss; 365 nm
406 excitation filter, 420 nm long pass (LP) barrier filter). Images were collected using the
407 AxioCamMRm camera and processed using the AxioVision 4.8 software (Zeiss).
408 Approximately 100 cells were measured from each data set (unless specified otherwise) using
409 the length tool within the Axiovision software.

410

411 **Coulter cytometer**

412 A volume of 100µL of fixed cells was added to 9.9mLs of Isoflow buffer (Beckman). Of this,
413 200µL was run through a 50µm aperture tube, and data collected over 400 bins ranging from
414 0.6 μm^3 to 100μm^3. Data was exported in excel and plotted as a histogram with the cell
415 volume along the x-axis and normalized cell counts on the y-axis, in Mathematica (Wolfram).
416 To compare the shift in cell size across all four biological replicates, the mode of each strain
417 from all replicates was calculated. The mode of wild-type expressing pBAD24 (short cells)
418 was set to 0% filamentation and the mode of wild-type expressing pBAD-*recA441*
419 (filaments) was set to 100% filamentation, to normalize all values. The modes of each mutant
420 strain across all four biological replicates were then combined to show the relative shift in
421 filamentation between strains.

422

423 **References**

424 1. Harry E, Monahan L, Thompson L. 2006. Bacterial cell division: the mechanism and
425 its precison. Int Rev Cytol 253:27-94.

426 2. Haeusser DP, Margolin W. 2016. Splitsville: structural and functional insights into
427 the dynamic bacterial Z ring. Nat Rev Microbiol 14:305-19.

428 3. den Blaauwen T, Hamoen LW, Levin PA. 2017. The divisome at 25: the road ahead.
429 Curr Opin Microbiol 36:85-94.

430 4. Adams DW, Wu LJ, Errington J. 2014. Cell cycle regulation by the bacterial
431 nucleoid. Curr Opin Microbiol 22:94-101.

432 5. Rowlett VW, Margolin W. 2015. The Min system and other nucleoid-independent
433 regulators of Z ring positioning. Front Microbiol 6:478.

434 6. Justice SS, Hunstad DA, Cegelski L, Hultgren SJ. 2008. Morphological plasticity as a
435 bacterial survival strategy. Nat Rev Microbiol 6:162-8.

436 7. Justice SS, Harrison A, Becknell B, Mason KM. 2014. Bacterial differentiation,
437 development, and disease: mechanisms for survival. FEMS Microbiol Lett 360:1-8.

438 8. Yang DC, Blair KM, Salama NR. 2016. Staying in Shape: the Impact of Cell Shape
439 on Bacterial Survival in Diverse Environments. Microbiol Mol Biol Rev 80:187-203.

440 9. Simmons LA, Foti JJ, Cohen SE, Walker GC. 2008. The SOS Regulatory Network.
441 EcoSal Plus 3.

442 10. Little JW. 1991. Mechanism of specific LexA cleavage: autodigestion and the role of
443 RecA coprotease. Biochimie 73:411-21.

444 11. Little JW. 1983. The SOS regulatory system: control of its state by the level of RecA
445 protease. J Mol Biol 167:791-808.

446 12. Janion C. 2008. Inducible SOS response system of DNA repair and mutagenesis in
447 Escherichia coli. Int J Biol Sci 4:338-44.

448 13. Butala M, Zgur-Bertok D, Busby SJ. 2009. The bacterial LexA transcriptional
449 repressor. Cell Mol Life Sci 66:82-93.
450 14. Huisman O, D'Ari R, Gottesman S. 1984. Cell-division control in Escherichia coli:
451 specific induction of the SOS function SfiA protein is sufficient to block septation.
452 Proc Natl Acad Sci U S A 81:4490-4.
453 15. Bi E, Lutkenhaus J. 1993. Cell division inhibitors SulA and MinCD prevent formation
454 of the FtsZ ring. J Bacteriol 175:1118-25.
455 16. Cordell SC, Robinson EJ, Lowe J. 2003. Crystal structure of the SOS cell division
456 inhibitor SulA and in complex with FtsZ. Proc Natl Acad Sci U S A 100:7889-94.
457 17. Justice SS, Garcia-Lara J, Rothfield LI. 2000. Cell division inhibitors SulA and
458 MinC/MinD block septum formation at different steps in the assembly of the
459 Escherichia coli division machinery. Mol Microbiol 37:410-23.
460 18. Dajkovic A, Mukherjee A, Lutkenhaus J. 2008. Investigation of regulation of FtsZ
461 assembly by SulA and development of a model for FtsZ polymerization. J Bacteriol
462 190:2513-26.
463 19. Chen Y, Milam SL, Erickson HP. 2012. SulA Inhibits Assembly of FtsZ by a Simple
464 Sequestration Mechanism. Biochemistry 51:3100-9.
465 20. Justice SS, Hunstad DA, Seed PC, Hultgren SJ. 2006. Filamentation by Escherichia
466 coli subverts innate defenses during urinary tract infection. Proc Natl Acad Sci U S A
467 103:19884-9.
468 21. Mizusawa S, Gottesman S. 1983. Protein degradation in Escherichia coli: the lon gene
469 controls the stability of sulA protein. Proc Natl Acad Sci U S A 80:358-62.
470 22. Haeusser DP, Hoashi M, Weaver A, Brown N, Pan J, Sawitzke JA, Thomason LC,
471 Court DL, Margolin W. 2014. The Kil peptide of bacteriophage lambda blocks

Escherichia coli cytokinesis via ZipA-dependent inhibition of FtsZ assembly. PLoS Genet 10:e1004217.

23. Heller DM, Tavag M, Hochschild A. 2017. CbtA toxin of Escherichia coli inhibits cell division and cell elongation via direct and independent interactions with FtsZ and MreB. PLoS Genet 13:e1007007.

24. Conter A, Bouche JP, Dassain M. 1996. Identification of a new inhibitor of essential division gene ftsZ as the kil gene of defective prophage Rac. J Bacteriol 178:5100-4.

25. Cam K, Bejar S, Gil D, Bouche JP. 1988. Identification and sequence of gene dicB: translation of the division inhibitor from an in-phase internal start. Nucleic Acids Res 16:6327-38.

26. Tan Q, Awano N, Inouye M. 2011. YeeV is an Escherichia coli toxin that inhibits cell division by targeting the cytoskeleton proteins, FtsZ and MreB. Mol Microbiol 79:109-18.

27. D'Ari R, Huisman O. 1983. Novel mechanism of cell division inhibition associated with the SOS response in Escherichia coli. J Bacteriol 156:243-50.

28. Maguin E, Brody H, Hill CW, D'Ari R. 1986. SOS-associated division inhibition gene sfiC is part of excisable element e14 in Escherichia coli. J Bacteriol 168:464-6.

29. Galkin VE, Yu X, Bielnicki J, Ndjonka D, Bell CE, Egelman EH. 2009. Cleavage of bacteriophage lambda cI repressor involves the RecA C-terminal domain. J Mol Biol 385:779-87.

30. Mehta P, Casjens S, Krishnaswamy S. 2004. Analysis of the lambdoid prophage element e14 in the E. coli K-12 genome. BMC Microbiol 4:4.

31. Burke C, Liu M, Britton W, Triccas JA, Thomas T, Smith AL, Allen S, Salomon R, Harry E. 2013. Harnessing single cell sorting to identify cell division genes and regulators in bacteria. PLoS One 8:e60964.

32. Mediati DG, Burke CM, Ansari S, Harry EJ, Duggin IG. 2018. High-throughput sequencing of sorted expression libraries reveals inhibitors of bacterial cell division. BMC Genomics 19:781.

33. Hu Z, Lutkenhaus J. 1999. Topological regulation of cell division in Escherichia coli involves rapid pole to pole oscillation of the division inhibitor MinC under the control of MinD and MinE. Mol Microbiol 34:82-90.

34. Hu Z, Mukherjee A, Pichoff S, Lutkenhaus J. 1999. The MinC component of the division site selection system in Escherichia coli interacts with FtsZ to prevent polymerization. Proc Natl Acad Sci U S A 96:14819-24.

35. Bernhardt TG, de Boer PAJ. 2005. SlmA, a Nucleoid-Associated, FtsZ Binding Protein Required for Blocking Septal Ring Assembly over Chromosomes in E. coli. Molecular Cell 18:555-564.

36. Schumacher MA, Zeng W. 2016. Structures of the nucleoid occlusion protein SlmA bound to DNA and the C-terminal domain of the cytoskeletal protein FtsZ. Proc Natl Acad Sci U S A 113:4988-93.

37. Baba T, Ara T, Hasegawa M, Takai Y, Okumura Y, Baba M, Datsenko KA, Tomita M, Wanner BL, Mori H. 2006. Construction of Escherichia coli K-12 in-frame, single-gene knockout mutants: the Keio collection. Mol Syst Biol 2:2006 0008.

38. Castellazzi M, George J, Buttin G. 1972. Prophage induction and cell division in E. coli. I. Further characterization of the thermosensitive mutation tif-1 whose expression mimics the effect of UV irradiation. Mol Gen Genet 119:139-52.

39. Wang WB, Tessman ES. 1985. Evidence that the recA441 (tif-1) mutant of Escherichia coli K-12 contains a thermosensitive intragenic suppressor of RecA constitutive protease activity. J Bacteriol 163:407-9.

40. Johnson JE, Lackner LL, de Boer PA. 2002. Targeting of (D)MinC/MinD and (D)MinC/DicB complexes to septal rings in Escherichia coli suggests a multistep mechanism for MinC-mediated destruction of nascent FtsZ rings. J Bacteriol 184:2951-62.

41. de Boer PA, Crossley RE, Rothfield LI. 1990. Central role for the Escherichia coli minC gene product in two different cell division-inhibition systems. Proc Natl Acad Sci U S A 87:1129-33.

42. Hernandez-Rocamora VM, Alfonso C, Margolin W, Zorrilla S, Rivas G. 2015. Evidence That Bacteriophage lambda Kil Peptide Inhibits Bacterial Cell Division by Disrupting FtsZ Protofilaments and Sequestering Protein Subunits. J Biol Chem 290:20325-35.

43. Khil PP, Camerini-Otero RD. 2002. Over 1000 genes are involved in the DNA damage response of Escherichia coli. Mol Microbiol 44:89-105.

44. Barshishat S, Elgrably-Weiss M, Edelstein J, Georg J, Govindarajan S, Haviv M, Wright PR, Hess WR, Altuvia S. 2018. OxyS small RNA induces cell cycle arrest to allow DNA damage repair. EMBO J 37:413-426.

45. Wang X, Kim Y, Ma Q, Hong SH, Pokusaeva K, Sturino JM, Wood TK. 2010. Cryptic prophages help bacteria cope with adverse environments. Nat Commun 1:147.

46. Harrison E, Brockhurst MA. 2017. Ecological and Evolutionary Benefits of Temperate Phage: What Does or Doesn't Kill You Makes You Stronger. Bioessays 39.

47. Dwyer DJ, Belenky PA, Yang JH, MacDonald IC, Martell JD, Takahashi N, Chan CT, Lobritz MA, Braff D, Schwarz EG, Ye JD, Pati M, Vercruysse M, Ralifo PS, Allison KR, Khalil AS, Ting AY, Walker GC, Collins JJ. 2014. Antibiotics induce

redox-related physiological alterations as part of their lethality. Proc Natl Acad Sci U S A 111:E2100-9.

48. Faith JJ, Hayete B, Thaden JT, Mogno I, Wierzbowski J, Cottarel G, Kasif S, Collins JJ, Gardner TS. 2007. Large-scale mapping and validation of Escherichia coli transcriptional regulation from a compendium of expression profiles. PLoS Biol 5:e8.

49. Kohanski MA, Dwyer DJ, Hayete B, Lawrence CA, Collins JJ. 2007. A common mechanism of cellular death induced by bactericidal antibiotics. Cell 130:797-810.

50. Datsenko KA, Wanner BL. 2000. One-step inactivation of chromosomal genes in Escherichia coli K-12 using PCR products. Proc Natl Acad Sci U S A 97:6640-5.

51. Gibson DG, Young L, Chuang RY, Venter JC, Hutchison CA, 3rd, Smith HO. 2009. Enzymatic assembly of DNA molecules up to several hundred kilobases. Nat Methods 6:343-5.

52. Addinall SG, Bi E, Lutkenhaus J. 1996. FtsZ ring formation in fts mutants. J Bacteriol 178:3877-84.

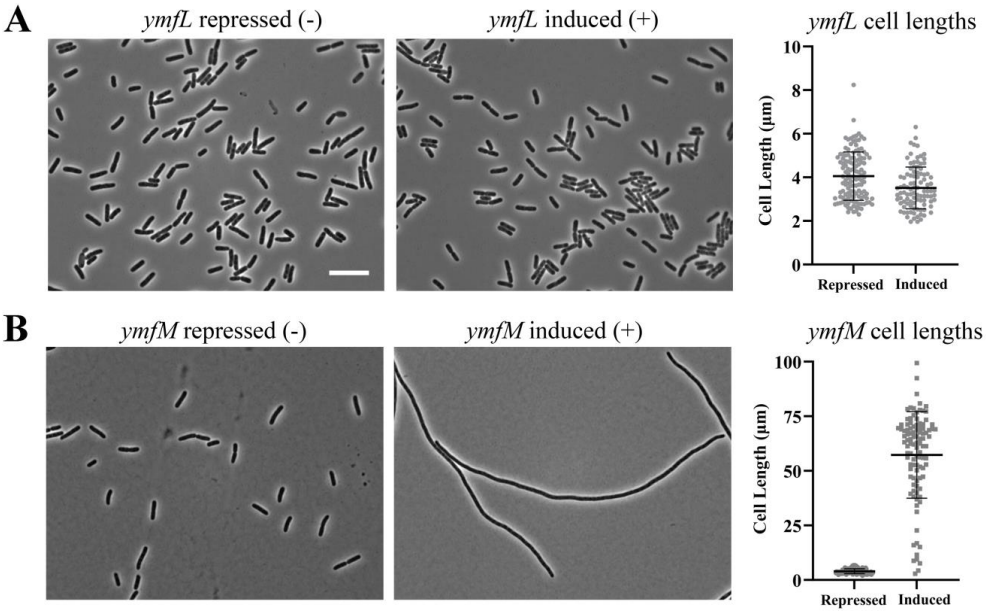

Figure 1. Cell length distribution when *ymfM* or *ymfL* is expressed from an inducible-plasmid

The open reading frame for genes (A) *ymfL* and (B) *ymfM* were cloned into the arabinose-inducible plasmid, pBAD24, and grown in LB medium, supplemented with 0.2% (w/v) glucose to repress their expression or 0.2% (w/v) arabinose to induce expression, for two

hours (4 generations). Representative phase-contrast image of induced *ymfM* expression shows filamentation of cells while the expression of *ymfL* does not affect cell length. Approximately 100 cells were measured for each population and cells lengths are shown on a scatterplot (error bars denote mean ± S.D) on the right. Scale bar for all images = 10µm

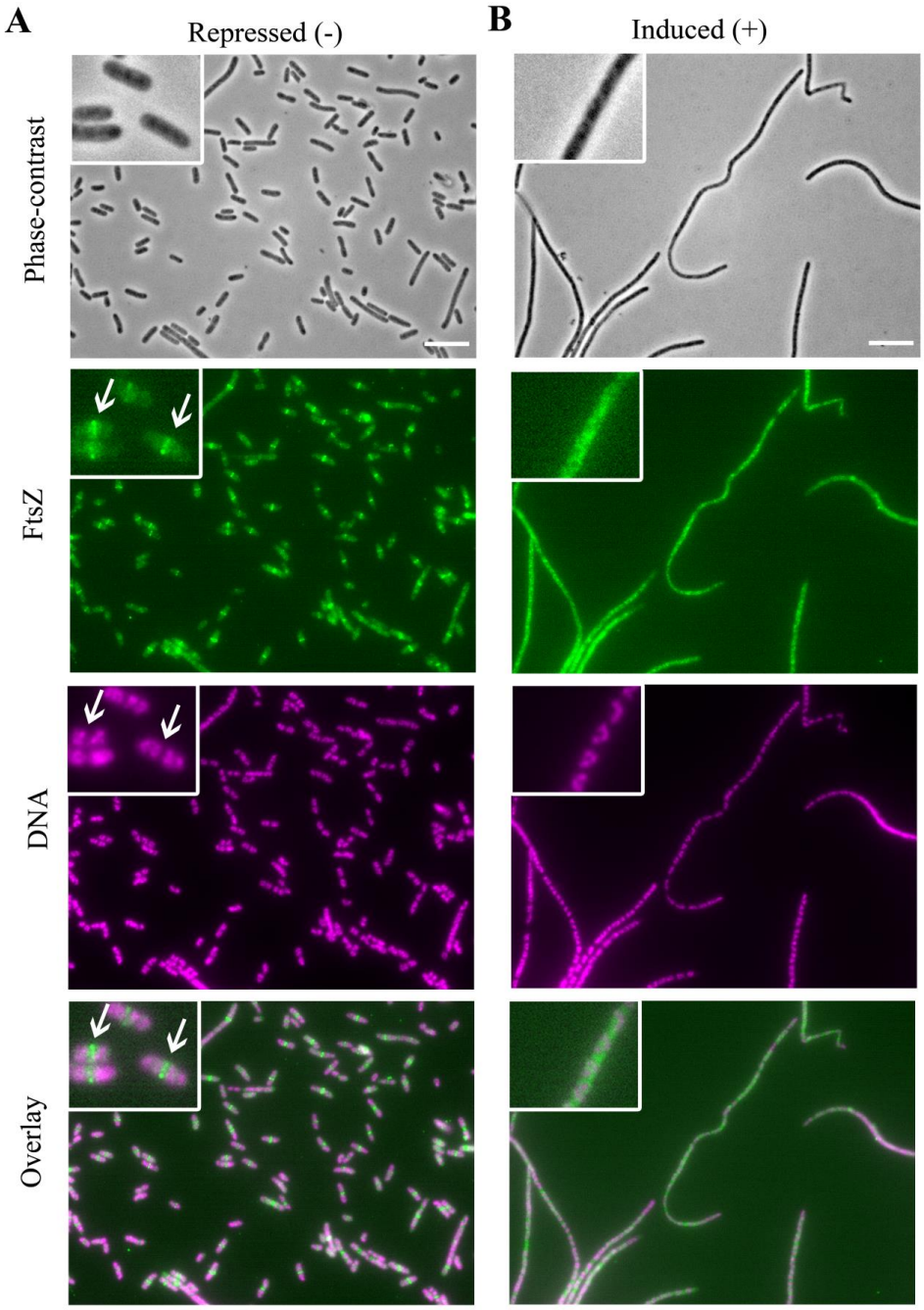

591

592 **Figure 2. Z ring assembly is inhibited in filamentous cells induced by *ymfM* expression**

593 Immunofluorescence microscopy using anti-FtsZ antiserum to visualize Z rings of strain

594 BW25113 carrying pBAD-*ymfM*. A) Cells grown in LB supplemented with 0.2% (w/v)

595 glucose to repress *ymfM* expression short cells are present with Z rings at mid-cell (white
596 arrows in inset indicate Z ring present as green bands). B) Expression of *ymfM* was induced
597 with 0.2% (w/v) arabinose for three generations (90 min) and the resulting filamentous cells
598 contain no Z rings. The nucleoids have been stained with DAPI (falsely coloured magenta)
599 and the overlay image shows Z-ring positioning within cells relative to nucleoids. Scale bars
600 for all images = 10µm.
601

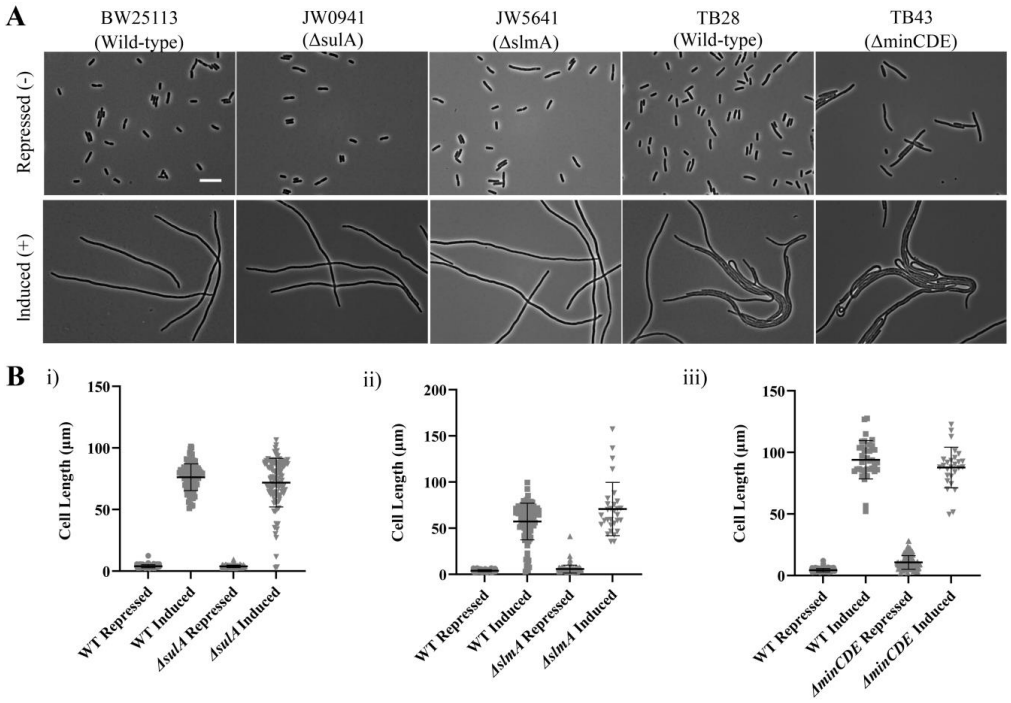

602

603 **Figure 3. Filamentation caused by the expression of *ymfM* is independent of the cell**

604 **division inhibitors, SulA, SlmA and the Min system.**

605 A) Phase-contrast images of strains, Δ*sulA* (JW0941), Δ*slmA* (JW5641), Δ*minCDE* (TB43)

606 and their wild-type backgrounds (BW25113 and TB28, respectively) show filamentation

607 when *ymfM* expression is induced from pBAD24 with 0.2% (w/v) arabinose in LB for two

608 hours (4 generations). Short cells are observed when *ymfM* expression is repressed with 0.2%

609 (w/v) glucose, with the exception of Δ*minCDE*, which has a mixed population of short,

610 slightly filamentous and minicells due to increased division at cell poles. B) Cell length

611 scatterplots of the mutants, (i) Δ*sulA*, (ii) Δ*slmA* and (iii) Δ*minCDE* show that the degree

612 filamentation caused by *ymfM* expression is comparable to their wild-type counterparts.

613 Approximately 100 cells were measured for each population and cells lengths are shown on a

614 scatterplot (error bars denote mean ± S.D) on the right. Scale bar for all images = 10μm

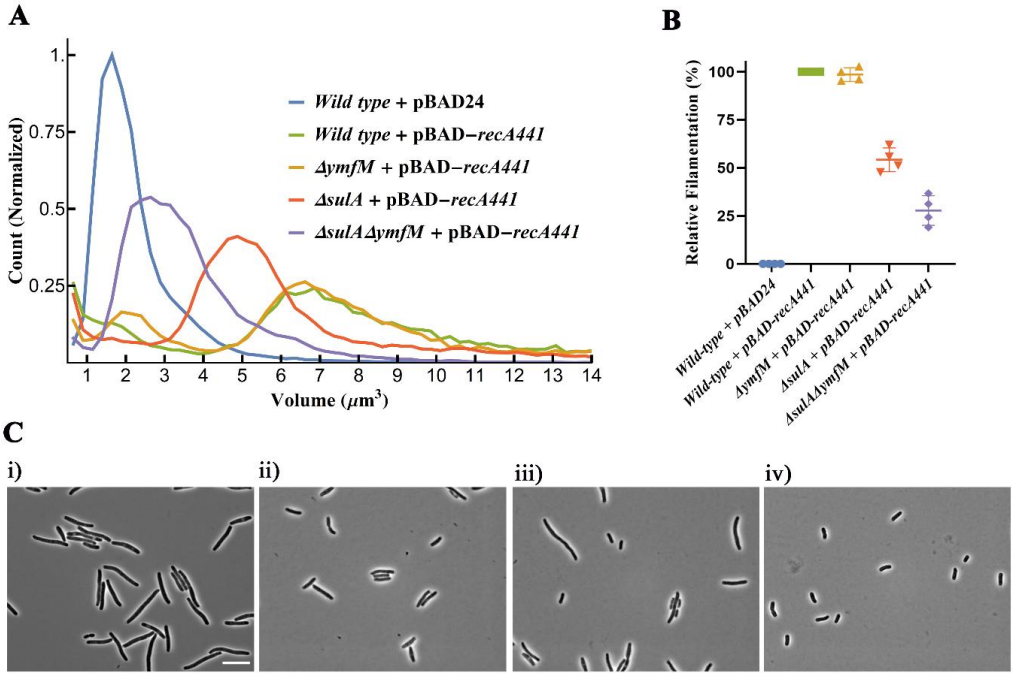

615

616 **Figure 4. YmfM contributes to the filamentation of *E. coli* during induction of the SOS**

617 **response using the temperature-sensitive RecA mutant, *recA441***

618 A) Coulter cytometer analysis of cell size distribution of wild-type (yellow), Δ*ymfM* (green),

619 Δs*ulA* (red), and Δs*ulA*Δ*ymfM* (purple) after two hours of pBAD-*recA441* induction in LB

620 with 0.2% (w/v) arabinose and 100 µg/mL adenine, at 42°C. Samples were compared to wild-

621 type cells expressing empty pBAD24 (blue) not under SOS induction. X-axis represents cell

622 volume (µm^3) and Y-axis represents cell count which has been normalized to 1. Pulse data >

623 10,000 events (cells). Data represents one biological replicate. Three additional biological

624 repeats were performed (Fig S4). B) The degree of filamentation of the mutant strains relative

625 to wild-type filaments. The data from four biological replicates has been normalised so that

626 mode of wild-type pBAD24 (short cells) is 0% and mode of wild-type pBAD-*recA441*

627 (filaments) is 100%. Error bars are mean ± S.D C) Representative phase-contrast image of

628 strains i) *wild-type* ii) Δ*sulA*, iii) Δ*ymfM* and, iv) Δ*sulA*Δ*ymfM*, all expressing pBAD-

629 *recA441*. Scale bar for all images = 10μm.